A METAL-DIELECTRIC MICRO-LINAC FOR RADIOGRAPHY SOURCE REPLACEMENT*

A. V. Smirnov†[1], S. Boucher[1], S. Kutsaev[1], R. Agustsson[2], R. Berry[2], K. Junge[2], J. Hartzell[2], J. McNevin[2], A. Murokh[2], E. Savin[2,3,#] and G. Leyh[4]
[1]RadiaBeam Systems, LLC, Santa Monica, CA 90404, USA
[2]RadiaBeam Technologies, LLC, Santa Monica, CA 90404, USA
[3]National Research Nuclear University (MEPhI), Moscow, 115409, Russia
[4]Lightning On Demand, Brisbane, CA, USA

Abstract

To improve public security and prevent the diversion of radioactive material for Radiation Dispersion Devices, RadiaBeam is developing an inexpensive, portable, easy-to-manufacture linac structure to allow effective capture of a ~13 keV electron beam injected from a conventional electron gun and acceleration to a final energy of ~ 1 MeV. The bremsstrahlung X-rays produced by the electron beam on a high-Z converter at the end of the linac will match the penetration and dose rate of a typical ~100 Ci or more Ir-192 source.

The tubular Disk-and-Ring structure under development consists of metal and dielectric elements that reduce or even eliminate multi-cell, multi-step brazing. This may allow significant simplification of the fabrication process to enable inexpensive mass-production required for replacement of the ~55,000 radionuclide sources in the US.

INTRODUCTION

Industrial linac systems are employed in a wide variety of applications, from radiography to sterilization. In general, such a conventional system consists of a low-gradient, usually S-band, linac with beam energy from a few to about ten MeVs, and average beam power in the range of few watts to 100 kW. As a rule these systems are rather expensive, bulky, heavy, and not portable. The MicroLinac technology originally developed at SLAC [1] employs a compact X-band linear accelerator powered by an inexpensive, low power, pulsed magnetron [2,3].

A considerable step forward has been made in the development of compact X-band MicroLinacs utilizing high-impedance, all-copper, multi-cell structures [2,4]. The biperiodic part of such a MicroLinac structure employs side [4] or on-axis [2] coupling cells enabling substantial number of cells sufficient to achieve beam energies exceeding 1 MeV within a single section at limited power supply (sub-MW in X-band). However, fabrication of a multi-cell, tapered MicroLinac structure remains a rather expensive and time consuming process not suitable for scaled-up production.

An attractive opportunity for eased fabrication of MicroLinac is using of dielectric loaded structures [5,6]. However, the practical implementation of a smooth-wall design is prevented by the single-wall multipactor effect [7] and charging of the dielectric material which causes damage at the required pulse repetition rates and beam currents. In a MicroLinac these problems are exacerbated by the high beam loss and low capture, as a continuous beam is injected from a thermionic injector at low energies (a few tens of keV). The shunt impedance over Q of a dielectric loaded structure at low phase velocity is noticeably lower compared to a conventional π-mode, iris loaded structure. This implies high permittivity for dielectrics, which is usually associated with elevated loss factors and thus further reduction of shunt impedance.

Our goal is to develop an easy-to-fabricate MicroLinac delivering ~1 MeV beam energy, 10 mA pulse current, 10 kW pulse power, and average beam power ~10 W. The initial concept of an X-band MicroLinac system for radiography source replacement is shown in Fig. 1. It employs a PM220 magnetron and M592 electron gun from L-3 and is powered by a light-weight, custom-built, Marx modulator.

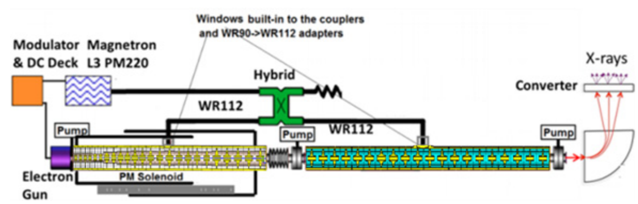

Figure 1: Conceptual scheme proposed for an X-band MicroLinac system for radiography source replacement.

DISK-AND-RING CELLS

Low-current, low-gradient applications benefit from simplified fabrication of the MicroLinac structure. We introduce here a hybrid metal-dielectric, periodic slow-wave structure. The novel Disk-and-Ring (DaR) cells are shown in Fig. 2 and Fig. 3.

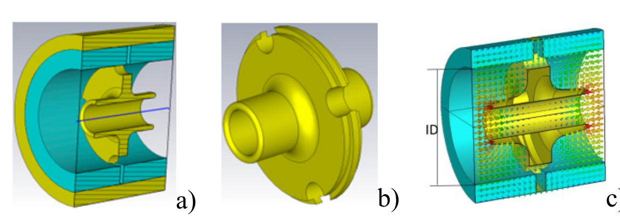

Figure 2: Compensated DaR cell for β_{ph}=0.94: cut view with Alumina rings (a), copper disk (b), and electric fields (c). Cell length 15 mm.

*Work supported by the U.S. Department of Energy (award No. DE-SC-FOA- SC0011370)
†asmirnov@radiabeam.com
On-leave from NRNU "MEPhI"

We use 0.75” standard copper tubing, 9.4 GHz operating frequency, and ∅3.175 mm beam aperture.

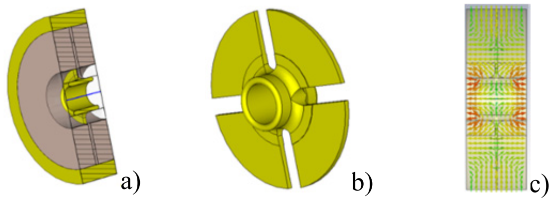

Figure 3: π-mode, β_{ph}=0.34 DaR cell cut view with Alumina rings (a), copper disk (b), and electric fields (c).

The design of a magnetic-type coupler requires presence of dielectrics across the coupling hole as shown in Fig. 4.

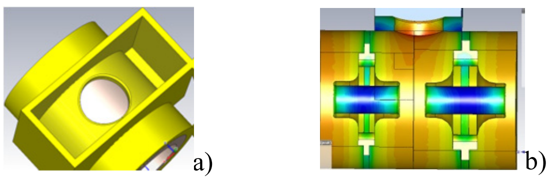

Figure 4: DaR coupler configuration (a) and surface current distribution (b).

MULTICELL STRUCTURE DESIGN

A multicell structure may combine both compensated [8] and non-compensated DaR cells. To exceed 1 MeV energy, we have initially designed two multi-cell accelerating structures shown in Fig. 5 with electric field Ez distributions given in Fig. 7.

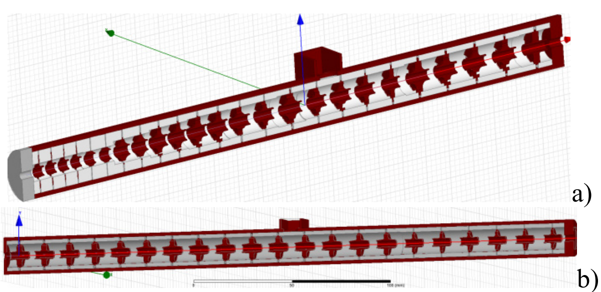

Figure 5: DaR MicroLinac sections: 13 keV-0.4 MeV (a) and (0.4-1.2)MeV (b).

The S11 parameter simulated in Fig. 6 indicates a significant (≥100 MHz) mode separation between the operating (geometrically-pure π-mode) and adjacent modes. This is more than an order of magnitude higher compared to a conventional π-mode X-band system.

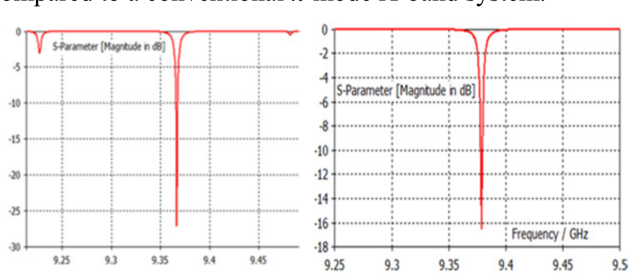

Figure 6: S11 parameter simulated for the operating modes (central peaks) of the DaR sections of Fig. 5.

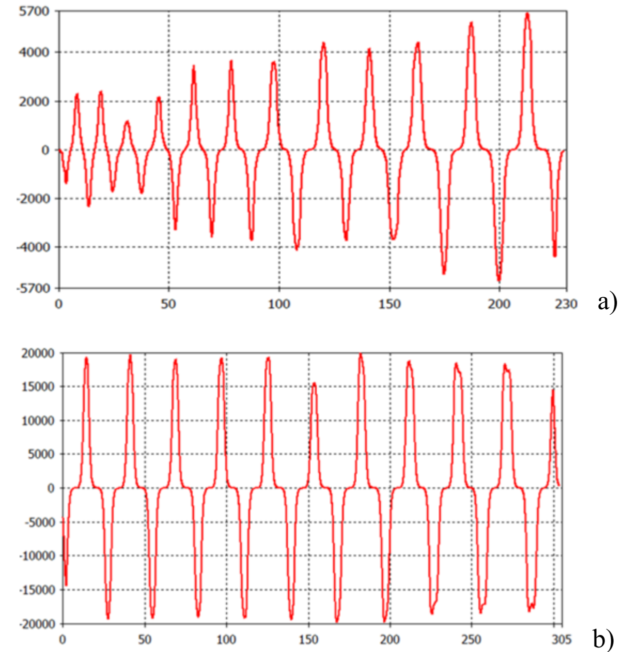

Figure 7: Longitudinal electric field profiles simulated along DaR MicroLinac for operating modes at ~9.4 GHz for the 1st (a) and 2nd (b) sections of Fig. 5.

This suggests that a longer section can be designed. An example of such a >1 MeV, 44-cell long structure is given in Fig. 8 and characterized in Fig. 9.

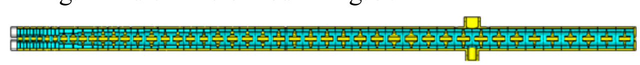

Figure 8: 44-cell DaR MicroLinac structure with RF (top) and evanescent vacuum ports (bottom).

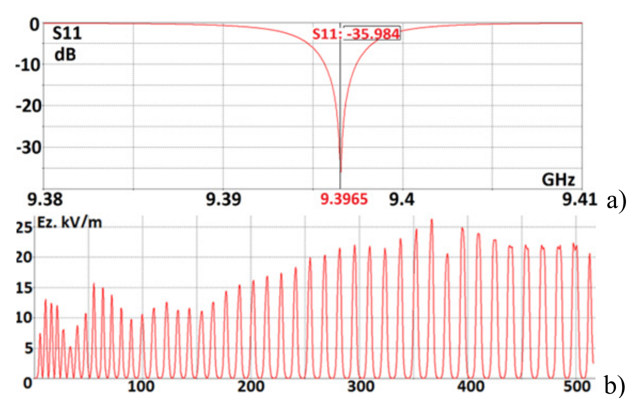

Figure 9: S11 parameter for DaR MicroLinac of Fig. 8 (a) and profile of the longitudinal electric field magnitude simulated at ~9.4 GHz (b).

BEAM DYNAMICS

Two focusing variants have been considered to confine most of the accelerated beam within the small 3 mm aperture. One variant utilizes the same solenoidal type focusing implemented with permanent magnet blocks in our prior MicroLinac designs [4]. ASTRA [9] simulation results for transverse and longitudinal beam dynamics are shown in Fig. 10 and Fig. 11 for the total RF power ~200 kW and 10^{-4} loss tangent.

ISBN 978-3-95450-147-2

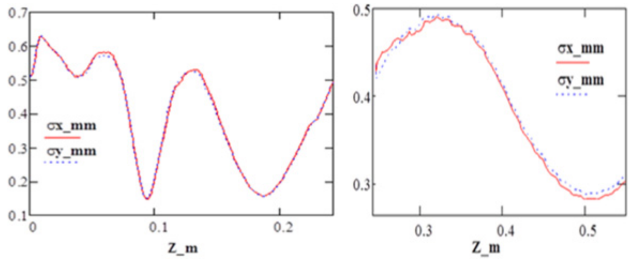

Figure 10: Beam rms transverse dimensions [mm] simulated along the 1st and 2nd sections of Fig. 4.

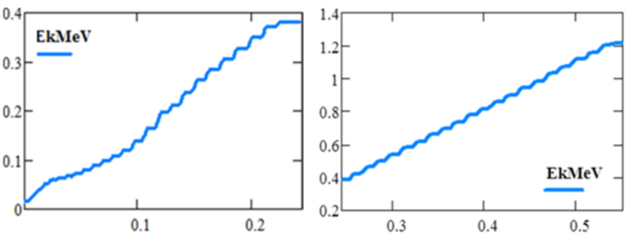

Figure 11: Beam kinetic energy [MeV] simulated along the 1st (left) and 2nd (right) sections [m].

Another focusing variant utilizes alternating periodic focusing. To our knowledge, so far it is used mostly in traveling wave tubes (TWTs). In particular we applied the focusing system shown in Fig. 12 built for the test mockup of (12-15) keV beam transport through the DaR structure.

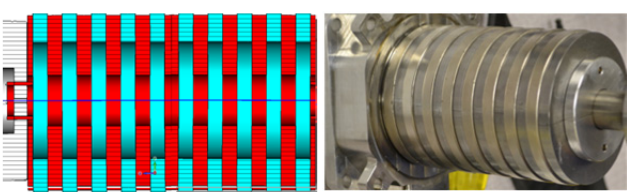

Figure 12: Alternating periodic focusing based on permanent magnet and mild steel rings. On-axis field magnitude: 0.17 T, period: 12 mm.

To show feasibility of this type of focusing we simulated in Fig. 12 beam dynamics along the short focusing section placed right after the injector.

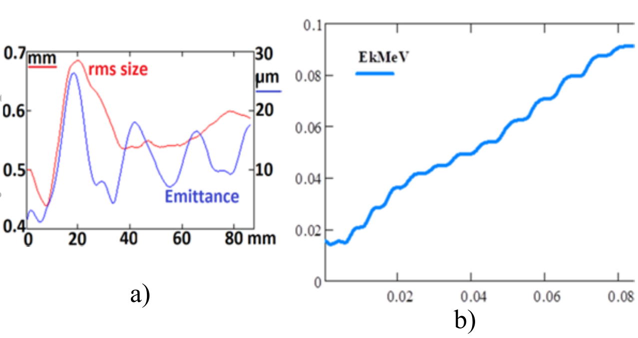

Figure 13: Beam rms sizes and normalized emittance (a) as well as energy gain (b) along the short focusing section of Fig. 12 and initial part of structure shown in Fig. 5a.

This initial part is important for beam capture, which can be as high as 40% and is driven by the matching region at the magnetic field entrance.

DISCUSSION

The dielectric part of the structure is isolated by the metal disks from the direct impact by the beam. Nevertheless the charging by the beam may affect the performance. This is expected to be dominated by charging of the disks. It can be mitigated by using a thin wire (pin) placed between the disk and the tubular housing or a thin conducting coating of the dielectric parts with a metal film having thickness much smaller than the skin depth (e.g., nanometers vs. ~700 nm skin depth in Copper in X-band). Note that, unlike the TiN coating used for multipactor suppression [7], the main function of such a coating is removal of static charge accumulated mostly on the disks.

As can be seen from Fig. 4, the RF port can in principle be combined with a vacuum window. This enables a vacuum-sealed, compact DaR tube variant (using built-in getter pumps).

A shorter version of the DaR structure can be also used to substitute Cobalt-57 source (115 keV X-rays).

ACKNOWLEDGMENT

This work was supported by the U.S. Department of Energy (award No. SC-FOA- SC0011370). The authors acknowledge Luigi Faillace for his results on gridded gun simulations and discussions.

REFERENCES

[1] N. Ackerman et al., “MicroLinac – A Portable Accelerator for Radiography”*, presented at the 12th Advanced Accelerator Concepts Workshop* (AAC’06)*,* Lake Geneva, Wisconsin, 2006, unpublished.

[2] T. Yamamoto et al., “Development of portable X-band linac X-ray source for non-destructive testing”, *in Proc. of the Joint Intern. Workshop: Nuclear Technology and Society–Needs for Next Generation*, Berkeley, California, 2008.

[3] S. Boucher, X. Ding, A. Murokh, *in Proc. of IPAC’10*, Kyoto, Japan, pp. 178-181, 2010.

[4] S. Boucher, R. Agustsson, L. Faillace, J. Hartzell, A. Murokh, A. Smirnov, S. Storms, K. Woods, *in Proc. of IPAC2013*, Shanghai, China, 2013, p. 3746.

[5] E. Chojnacki et al., “Measurement of deflection-mode damping in an accelerating structure”, *J. Appl. Phys*., vol. 69, pp. 6257-6260, 1991.

[6] P. Zou et al., “Construction and testing of an 11.4 GHz dielectric structure based traveling wave accelerator”, *Rev. Sci. Instrum*., vol. 71, pp. 2301–2304, 2000.

[7] C. Jing, J. G. Power, et al.*, in Proc. of PAC’05*, paper TPAE017, Knoxville, Tennessee, pp. 1566-1569, 2005.

[8] A. V. Smirnov and E. Savin, “Hybrid metal-dielectric, slow wave structure with magnetic coupling and compensation”, *Nuclear Inst. and Meth. NIM A*, vol. 820, N1 (2016) pp. 48-53.

[9] Astra - A space charge tracking algorithm. User’s manual. Version 3.0, DESY, Hamburg, 2011.